Plasmonic Nanostructured Cellular Automata

Emad Alkhazraji[1,*], *A. Ghalib*[2], *K. Manzoor*[2] *and M. A. Alsunaidi*[2]

[1]Jubail Industrial College, Jubail 31961, Saudi Arabia
[2]King Fahd University of Petroleum & Minerals, Dhahran 31261, Saudi Arabia

Abstract. In this work, we have investigated the scattering plasmonic resonance characteristics of silver nanospheres with a geometrical distribution that is modelled by Cellular Automata using time-domain numerical analysis. Cellular Automata are discrete mathematical structures that model different natural phenomena. Two binary one-dimensional Cellular Automata rules are considered to model the nanostructure, namely rule 30 and rule 33. The analysis produces three-dimensional scattering profiles of the entire plasmonic nanostructure. For the Cellular Automaton rule 33, the introduction of more Cellular Automata generations resulted only in slight red and blue shifts in the plasmonic modes with respect to the first generation. On the other hand, while rule 30 introduced significant red shifts in the resonance peaks at early generations, at later generations however, a peculiar effect is witnessed in the scattering profile as new peaks emerge as a feature of the overall Cellular Automata structure rather than the sum of the smaller parts that compose it. We strongly believe that these features that emerge as a result adopting the different 256 Cellular Automata rules as configuration models of nanostructures in different applications and systems might possess a great potential in enhancing their capability, sensitivity, efficiency, and power utilization.

1 Introduction

Cellular Automaton (CA) theory was established and developed in the second half of the last century [1]. A one-dimensional Cellular Automaton is a discrete mathematical structure that is consisted of a sequence of k number of consecutive cells where each cell can take a value between 0 and $k-1$. The initial state of the structure is dubbed as the first generation or generation 0. Thereafter, the value of each cell is updated in accordance with the cell's present value and its neighbouring cells' values as determined by a specific rule set that is depicted by each of the available 256 CA rules as generations progress. The decimal value of each rule is represented in hexadecimal form and then the binary equivalent of this hexadecimal number associates with different combinations of input values of the cells [1, 3]. Cellular Automata had been extensively used in several applications, such as image processing, traffic modelling, and music composition [2]. Furthermore, different CA can model several universal dynamic phenomena and occurrences ranging from DNA sequences to galactic formations [3].

We believe that employing these nature-complying rules as configuration models in different artificial systems and structures, such as sensing, imaging, and energy harvesting applications, can introduce positive enhancements to their capabilities, efficiencies, and energy utilization. In this work, we investigate the scattering plasmonic resonance profiles of silver spherical nano-particles when CA rules are used as models of their geometrical distribution. Thereafter, we characterize the scattering profiles of these CA configurations while observing how they evolve after each generation.

2 Analysis model

The analysis model of this study is based on the numerical time-domain solution of Maxwell's equations for electrodynamics, where scattering light waves inside the nanostructure is simulated and analyzed. As such, a three-dimensional TMz domain was implemented where the electric and magnetic fields are represented in a finite-difference time-domain scheme according to Yee's 3D staggered mesh. To eliminate the effect of reflections from the finite numerical domain, the generalized material-independent perfect matching layer (GMIPML), introduced in [4], was implemented at all boundaries with a thickness of eight mesh cells. In addition, two different techniques have been used in order to isolate and find the scattered fields and to simulate the dispersive nature of the silver nanospheres.

2.1 Total-fields/scattered-fields

Total-Field/Scattered-Field (TF/SF) technique is used to identify the scattered waves of different scattering objects inside the established domain and to isolate them from the source wave fields. Inside the whole domain, a closed region is defined inside which, the targeted object is cantered. Inside this region, both incident source fields and scattered fields, off the target, are present hence, it is

called the Total Region. Outside that region, however, by eliminating the incident fields' components, the scattered fields are isolated and tracked as time progresses. This region is called the Scattered Region.

In order to characterize the scattering plasmonic profile of any structure, the poynting vector of the scattered waves are calculated as a function of time at all sides of the three-dimensional domain. Finally, taking the Fourier transform of the scattered power generates the scattering resonance profile of the target where the peaks of the profile represent the scattering plasmon modes of the scattering target.

2.2 Simulation of Dispersive Nature of Silver

The General Algorithm proposed in [5] is used to model the dispersive nature of the plasmonic nano-structures. Following Lorentz–Drude model, the polarization vector P for each pole can be obtained using

$$P^n = \frac{4}{2+\tau_i \Delta t} P^{n-1} - \frac{2-\tau_i \Delta t}{2+\tau_i \Delta t} P^{n-2} + \frac{2\epsilon_o f_i \omega_i^2 \Delta t^2}{2+\tau_i \Delta t} E^{n-1} \quad (1)$$

where n represents the time step while τ_i, ω_i, and f_i are the pole parameters. Thereafter, the electric fields are updated using

$$E^n = \frac{D^n - \sum_i^N P_i^n}{\varepsilon_0 \varepsilon_\infty} \quad (2)$$

where D is the electric flux density and N is the number of poles which is 6 in the case of silver whose corresponding poles' parameters were obtained from [6].

3 Implementation of CA rules

Two binary one-dimensional CA, namely CA 30 and CA 33, have been adopted to model the spatial distribution of the silver nanospheres which have been distributed over a plane that is normal to the direction of propagation of the incident light wave. Each generation is 11 cells-wide where each cell can take either a value of 0 or 1 dictating the absence or the presence of a nanosphere in that cell location, respectively. The radius of the nanospheres was 5 nm with a separation of 1 nm.

3.1 Cellular Automaton 33

Cellular Automaton rule 33 is a simple one-dimensional non-divergent CA rule [7]. Fig.1 shows the first 10 generations of that rule for a width of 11 cells/generation. To follow this CA rule as a model, initially, the first generation was implemented by deploying a single sphere (see inset of Fig. 2) at the top middle of the total region inside the domain. The scattering profile of this configuration, as shown in Fig. 2, is consisted of two resonance wavelengths, which matches that of a typical silver nanosphere [8,9], as represented by the peaks at 257 nm and 378 nm, respectively.

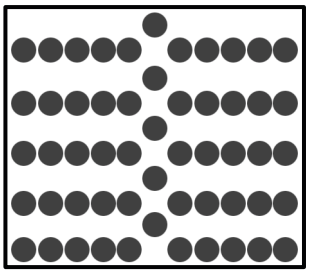

Fig. 1. CA rule 33 after 10 generations of a width of 11 cells.

Thereafter, going in generation-by-generation for 10 generations, more silver nanospheres have been added according to CA rule 33 as shown in Fig. 1. After each generation, the scattering profile had been found to be similar to that of first generation albeit with a slight red or blue shift in both peaks as generations progressed.

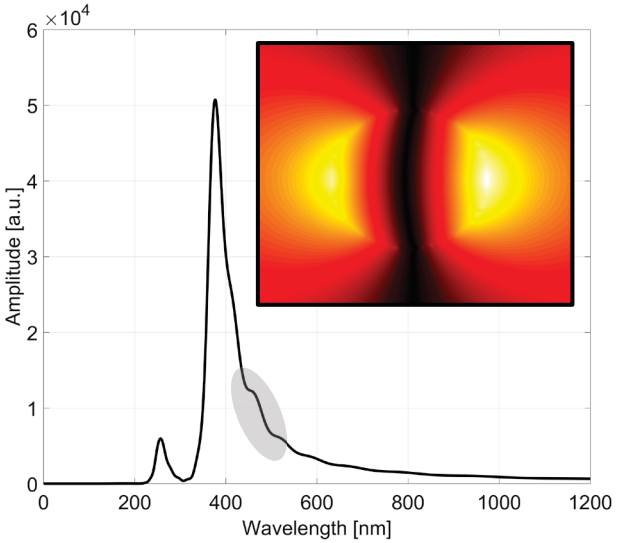

Fig. 2. Scattering profile of the first generation that is consisted of a single nanosphere (inset).

3.2 Cellular Automaton 30

Cellular Automaton 30, much like CA 33, is a one-dimensional CA whose cells can occupy one of two states. The inset in Fig. 3 shows the first eight generations of this rule for a width of 15 cells/generation. More interestingly, this CA rule is mostly known for its chaotic nature as it is classified as a class III CA rule and, hence, is used in random number generators. Moreover, some natural phenomena can be modelled by this rule such as patterns on seashells and other creatures [10].

Starting with an identical first generation to that of CA 33, eight generations of CA 30 were implemented one after another each with a width of 15 cells. Fig. 3 shows a side and a top view (left to right) of the configuration after the eighth generation in plasmonic resonance.

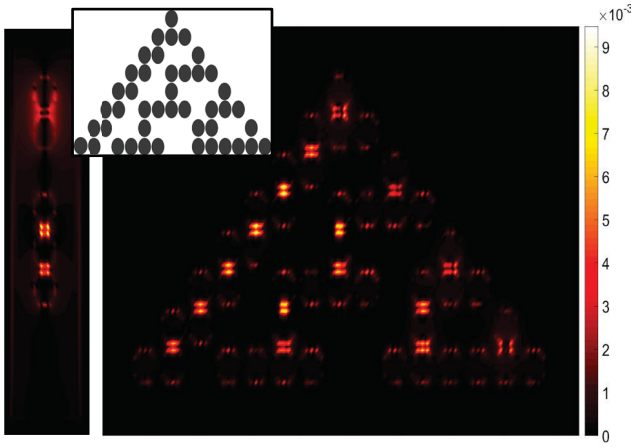

Fig. 3. A side and a top view (left to right) of CA 30 after 8 generations. The inset illustrates the first eight 15-cell-wide generations of that rule.

After adding the second and third generations, the effect on the scattering profile was similar to that of CA 33 where slight shifts were observed in both modes of the profile. However, after introducing the fourth generation, a very peculiar anomaly is witnessed in the scattering profile as a new peak emerges at a wavelength of 463 nm as shown in Fig. 4 by the solid curve. Furthermore, the newly added particles in the fourth generation alone were isolated and their scattering profile was acquired. This was done in order to investigate the newly emerged mode and identify whether its appearance is attributed to the structure itself or if it is merely a sum of its parts. Surprisingly enough, as Fig. 4 demonstrates, the profile of the isolated nanospheres that were introduced in the fourth generation (represented by the dashed curve) matched that of the of the structure after 3 generations (represented by the dotted curve). This indicates that indeed the Cellular Automaton structure itself is introducing its own new features rather than a mere superposition of its composing elements.

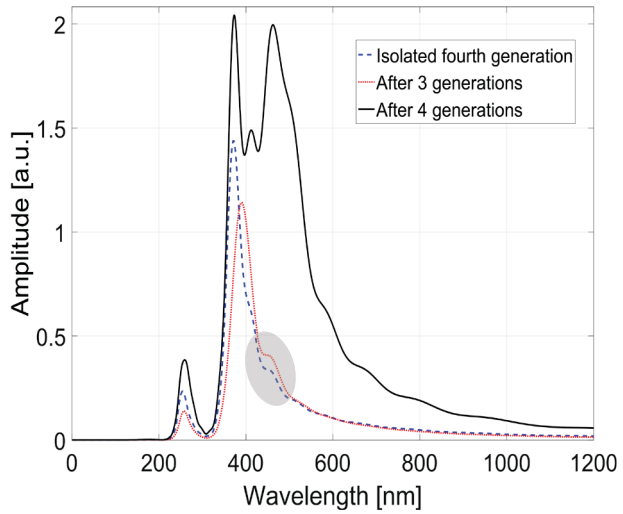

Fig. 4. Side-by-Side comparison between the scattering profiles of the CA 30 structure after 3 generations (dotted curve) and after 4 generations (solid curve), and of the isolated newly added nanoshperes in the fourth generation alone (dashed curve).

Furthermore, in all prior scattering profiles, a small hump was observed (shaded regions in Figs. 2 and 4) around the particular wavelength where the new peak has emerged. We postulate that the Cellular Automaton configuration is enhancing the plasmons of the collective nanospheres at the hump and is enabling it to become a fully-fledged resonance mode.

4 Conclusion

Two Cellular Automata have been implemented as models of distribution of silver nanospheres whose scattering profiles were acquired after each generation. While Cellular Automaton rule 33 is a simple and a systematic rule, which provides simplicity and ease of implementation, it showed a scattering profile matching that of a single silver nanosphere with two resonance modes that blue and red shift as more generations are introduced. On the other hand, Cellular Automaton rule 30 is a chaotic and a divergent rule which introduces difficulties and limitations in design and implementation. Whilst the first few generations showed a similar profile to CA 33, the later generations, however, introduced a new mode that was accredited to the CA 30 configuration itself as it enhanced the plasmonic scattering at that particular mode. A new scattering resonance mode can be directly correlated to providing an extra degree of sensing capabilities in bio-sensing or chemical sensing as some features of the sensing target can be translated by either a shift or change in the response waist size in any of these modes.

With all said and done, there is a total of 254 Cellular Automata besides the two which were used in this work. This study only scratches the surface of the great potential that we believe can be achieved by the adoption of these universal dynamic structures as models in our different artificial applications and systems of nanostructures that can enhance their capabilities, sensitivities, and efficiencies.

References

1. S. Wolfram. "*Cellular Automata as models of complexity*," Nature, **311**, 419-424 (Oct. 1984)
2. D. Das. "*A survey on Cellular Automata and its application,*" Global Trends in Computing and Communication Systems, Berlin Heidelberg: Springer, 753-762 (2012)
3. K. Fujibayashi, R. Hariadi, S. Park, E. Winfree, and S. Murata. "*Toward reliable algorithmic self-assembly of DNA tiles: a fixed-width Cellular Automaton pattern,*" Nano Letters **8(7)**, 1791-1797 (2007)
4. A.P. Zhao, J. Juntunen, A.V. Raisanen. "*Generalized material-independent PML absorbers for the FDTD simulation of electromagnetic waves in arbitrary anisotropic dielectric and magnetic media,*" Microwave and Guided Wave Letters, IEEE, **8(2)**, 52-54 (1998)

5. A. Al-Jabr, M. A. Alsunaidi. "*An efficient time-domain algorithm for the simulation of heterogeneous dispersive structures*," Journal of Infrared, Millimeter, and Terahertz Waves, **30**, 1226-1233 (2009)
6. A. D. Rakic, A. B. Djurisic, J. M. Elazar, M. L. Majewski. "*Optical properties of metallic films for vertical cavity optoelectronic devices,*" Appl. Opt., **37**, 5271–5283 (1998)
7. W. Eric. "Elementary Cellular Automaton," (2015) URL: www.mathworld.wolfram.com/ElementaryCellularAutomaton.html
8. V. Yannopapas, N.V. Vitanov. "Ultra-subwavelength focusing of light by a monolayer of metallic nanoshells with an adsorbed defect," RRL, **2(6)**, 287-289 (2008)
9. M. K. Schmidt, R. Esteban, J. Sáenz, I. Suárez-Lacalle, S. Mackowski, J. Aizpurua. "Dielectric antennas-a suitable platform for controlling magnetic dipolar emission," Optics express, **20(13)**, 13636-13650 (2012)
10. Weisstein, W. Eric. "Rule 30." (2011) URL: www.mathworld.wolfram.com/Rule30.html